

2  
CENF-760647--2

RECEIVED BY TIC JUL 1 1976

PREPRINT UCRL-78268

## Lawrence Livermore Laboratory

MEASUREMENTS OF NEUTRON-INDUCED FISSION  
CROSS-SECTION RATIOS INVOLVING ISOTOPES  
OF URANIUM AND PLUTONIUM

J. W. Behrens

G. W. Carlson

June 8, 1976

This paper was prepared for the NEANDC/NEACRP Specialists  
Meeting on Fast Neutron Fission Cross Sections of  $^{233}\text{U}$ ,  
 $^{235}\text{U}$ ,  $^{238}\text{U}$ , and  $^{239}\text{Pu}$ , June 28-30, 1976,  
Argonne, Illinois 60439.

This is a preprint of a paper intended for publication in a journal or proceedings. Since changes may be made before publication, this preprint is made available with the understanding that it will not be cited or reproduced without the permission of the author.



MASTER

RECEIVED BY TIC JUL 1 1976

DISTRIBUTED

DOCUMENT IS UNLIMITED

NOTICE

This report was prepared in the course of work sponsored by the United States Government. Neither the United States nor the United States Energy Research and Development Administration nor any of their employees, or any of their contractors, subcontractors, or their employees, makes any warranty, express or implied, as to the quality, reliability, or acceptability for the accuracy, completeness or usefulness of any information, apparatus, product or process disclosed, or represents that its use would not infringe privately owned rights.

## MEASUREMENTS OF NEUTRON-INDUCED FISSION CROSS-SECTION RATIOS INVOLVING ISOTOPES OF URANIUM AND PLUTONIUM

J. W. Behrens and G. W. Carlson

Lawrence Livermore Laboratory, University of California  
Livermore, California 94550 USA

### ABSTRACT

A procedure, called the threshold cross-section method was applied to our experimental data involving our uranium ( $^{233}\text{U}$ ,  $^{234}\text{U}$ ,  $^{236}\text{U}$ , and  $^{238}\text{U}$ ) and five plutonium ( $^{239}\text{Pu}$ ,  $^{240}\text{Pu}$ ,  $^{241}\text{Pu}$ ,  $^{242}\text{Pu}$ , and  $^{244}\text{Pu}$ ) isotopes to determine ratios of fission cross sections relative to  $^{235}\text{U}$ . The data were gathered using ionization fission chambers and the time-of-flight technique at the LLL 100-MeV electron linear accelerator; measurements span the neutron energy range of 0.001 to 30 MeV. Experimental uncertainties common to past measurements were either eliminated or significantly reduced in this study by use of the threshold method, thereby making higher accuracies possible. Our cross-section ratios are absolute in the sense that they do not depend on the work of others. Results from our ratios involving  $^{233}\text{U}$ ,  $^{235}\text{U}$ ,  $^{238}\text{U}$ , and  $^{239}\text{Pu}$  are used to illustrate this method.

### INTRODUCTION

Over the past two decades, many measurements of the neutron-induced fission cross-section ratios involving isotopes of uranium and plutonium have been published. In most cases, these ratios are made with respect to the fission cross section of  $^{235}\text{U}$ , and fall into two categories: ratios in which the measurement includes an experimental means for determining the normalization, and ratios that are arbitrarily normalized to a value taken from either another experiment or from an evaluation. Ratios belonging to the first category not only give definition to the relative energy dependence of the cross sections but also provide an independent means for obtaining absolute fission cross sections once the cross section of the reference nuclide is known. Fission cross-section ratio measurements involving the relatively long-lived isotopes of uranium ( $^{233}\text{U}$ ,  $^{234}\text{U}$ ,  $^{235}\text{U}$ ,  $^{236}\text{U}$ , and  $^{238}\text{U}$ ) and plutonium ( $^{239}\text{Pu}$ ,  $^{240}\text{Pu}$ ,  $^{241}\text{Pu}$ ,  $^{242}\text{Pu}$ , and  $^{244}\text{Pu}$ ) were recently completed at LLL using our threshold cross-section method.

Our measurements were conducted using ionization fission chambers and the time-of-flight technique at the LLL 100-MeV electron linear accelerator

49

(linac). The measurements span the neutron energy range of 0.001 to 30 MeV, except where limited by low cross sections in the threshold isotopes. The continuous energy spectrum of the neutron source allowed us to cover the entire energy range of each ratio in one measurement. In this paper our experimental setup and techniques are summarized and references containing more detailed information about our experiment as well as listings of some of our data are given. This work emphasizes the threshold cross-section method as outlined earlier by Behrens [1], and a comparison with the commonly used method illustrates the elimination or significant reduction of experimental uncertainties that is possible with our procedure.

#### EXPERIMENTAL PROCEDURE

##### Neutron Source and Detectors

Most of the measurements were conducted with fission chambers located at the 34.3-m station of the 250-m time-of-flight tube at the LLL linac. The ratios involving  $^{240}\text{Pu}$ ,  $^{242}\text{Pu}$ , and  $^{244}\text{Pu}$  were measured at 15.8 m to reduce the effect of spontaneous fission backgrounds. The linac was operated at 1440 Hz with an electron pulse width of 10 ns to produce neutrons in a water-cooled tantalum target.

The fission detectors were parallel-plate ionization chambers of modular design, placed back-to-back in a pressure vessel with the foils oriented perpendicular to the incident neutron beam. Both time-of-flight and pulse-height information were processed for each event in our data acquisition system. Table I lists the isotopic compositions and areal densities of our high-purity fissionable materials.

##### Timing, Resolution, and Backgrounds

The gamma flash from the tantalum target was used as our main timing reference for most of our measurements. We verified this timing by measuring the positions of the MeV resonances of carbon and our time-of-energy conversion includes the relativistic correction.

The resolution of our experiment was determined by the resolution of the fission detector (<9 ns) and the pulse width of the electron pulses striking the tantalum target ( $\sim$ 10 ns). Uncertainty in flight path as well as in finite target and detector thickness resulted in a loss of resolution that was small compared to the magnitude of these two components. Our data have typical energy resolutions of 6% at 20 MeV and 1.5 to 3.0% at 1 MeV.

Out-of-time neutron backgrounds were measured at both time-of-flight stations using the black-resonance absorber technique and were found to contribute negligible error (<0.1%). Time-independent backgrounds resulting from amplifier noise, alpha pileup pulses, and spontaneous fission were subtracted and, in most cases, these corrections also contributed negligible error. A variety of reports further describing our experiment and experimental errors are available [2-7]; several contain listings of our data [4,6,7].

### Comparison of Procedures for Determination of Cross-Section Ratios

A common procedure for fission cross-section ratio determination requires the placement of fission detectors, each containing a high-purity fissionable isotope, such that they are run simultaneously in the same neutron flux. The expected counting rates in these detectors are then

$$r_A(E) = \phi(E)N_A\sigma_A(E) \quad \text{and} \quad r_B(E) = \phi(E)N_B\sigma_B(E),$$

where  $\phi(E)$  is the neutron flux and  $N_A$  and  $N_B$  are the numbers of atoms of isotopes A and B. The ratio of these rates gives

$$\frac{r_A(E)}{r_B(E)} = \frac{N_A\sigma_A(E)}{N_B\sigma_B(E)} \quad \text{or} \quad \frac{\sigma_A(E)}{\sigma_B(E)} = \frac{N_B}{N_A} \frac{r_A(E)}{r_B(E)}.$$

The atom ratio,  $N_B/N_A$ , must be known to determine the fission cross-section ratio,  $\sigma_A(E)/\sigma_B(E)$ . In practice, the fission detectors usually have different fission fragment detection efficiencies that are less than 100% because of fragment losses in the fission foils and other effects. Thus, to account for detector efficiencies, the expression becomes

$$\frac{\sigma_A(E)}{\sigma_B(E)} = \frac{\beta_B N_B}{\beta_A N_A} \frac{r_B(E)}{r_A(E)},$$

where  $\beta_A$  and  $\beta_B$  are the explicit detector efficiencies, and the ratio  $\beta_B N_B / \beta_A N_A$  is the "effective" atom ratio. The measurement must now include either the determination of  $\beta_A$  and  $\beta_B$  or the determination of the effective atom ratio, itself. Efficiencies are usually determined by studying the pulse-height distributions and estimating the fragment losses. The effective atom ratio is usually measured at a neutron energy where the cross-section ratio is assumed to be well-known, e.g., at thermal neutron energy. Experimental uncertainties arising from these added steps can dominate the list of errors and limit the accuracy of the final cross-section ratio. Some investigators indicate that the determination of the effective atom ratio is the critical problem that limits the accuracy of the entire measurement [8,9]. The numbers of atoms,  $N_A$  and  $N_B$ , can be determined by assaying techniques such as alpha counting, isotope-dilution mass spectrometry, and controlled-potential coulometry. The errors associated with these techniques further limit the accuracy of the final result. In recent years this commonly-used procedure has been used in a variety of published fission cross-section ratio measurements with considerable emphasis placed on the discussion of detector efficiencies, fragment losses, and assaying techniques [8-16].

Our data were reduced using a procedure we call the threshold cross-section method. With this method it is possible to obtain results with total uncertainties of less than 1% for each threshold-isotope ratio. Determination of ratios involving two nonthreshold isotopes can be accomplished by using this method more than once, as illustrated in the next section.

The threshold method uses two fission chambers. The first contains a mixture of the two isotopes of interest with an atom ratio,  $\eta$ , of the isotope B to the threshold isotope A. For some range of energies below the threshold

of isotope A, the ratio of fission cross sections,  $\sigma_A(E)/\sigma_B(E)$ , must be negligible when compared with the same ratio above the threshold. The expected counting rate in the mixed chamber is

$$r_m(E) = \phi(E) \beta_m N_A \{ \sigma_A(E) + n \sigma_B(E) \} ,$$

where  $\phi(E)$  is the neutron flux,  $N_A$  is the number of atoms of isotope A, and  $\beta_m$  is the efficiency for detecting fission fragments in the mixed chamber. The second fission chamber contains  $N_B$  atoms of pure isotope B and has an efficiency of  $\beta_p$ . The counting rate for this pure chamber is

$$r_p(E) = \phi(E) \beta_p N_B \sigma_B(E) .$$

To measure  $r_m(E)$  and  $r_p(E)$ , the two chambers are exposed simultaneously to the same neutron beam. The ratio of their rates gives

$$R(E) = \frac{r_m(E)}{r_p(E)} = \frac{\beta_m N_A}{\beta_p N_B} \left( \frac{\sigma_A(E)}{\sigma_B(E)} + n \right) .$$

Below the threshold of isotope A,  $R(E)$  is a constant,  $Q$ , and the experimental results yield the ratio of the effective numbers of atoms since

$$\frac{\beta_m N_A}{\beta_p N_B} = \frac{Q}{n} .$$

Substituting  $Q/n$  into the above equation and solving for  $\sigma_A(E)/\sigma_B(E)$ , we obtain the cross-section ratio,

$$\frac{\sigma_A(E)}{\sigma_B(E)} = n \left( \frac{R(E)}{Q} - 1 \right) . \quad (1)$$

Only the atom ratio in the mixed chamber,  $n$ , is a necessary prerequisite in the determination of the cross-section ratio.

#### RESULTS OBTAINED USING THE THRESHOLD METHOD

Application of the threshold method to the determination of the  $^{238}\text{U}/^{235}\text{U}$  fission cross-section ratio will further illustrate this procedure. In this measurement the mixed chamber, containing a homogeneous mixture of  $^{235}\text{U}$  and  $^{238}\text{U}$ , was prepared from materials of high isotopic purity. The atom ratio,  $n$ , of the  $^{235}\text{U}$  isotope to the threshold isotope,  $^{238}\text{U}$ , was determined using mass spectrometry. The pure chamber contained high-purity  $^{235}\text{U}$  and both chambers were exposed simultaneously to the same neutron beam. The ratio,  $R(E)$ , of the counting rates  $r_m(E)$  and  $r_p(E)$ , taken from one of our experimental runs, is shown in Figure 1a. Below the threshold of the  $^{238}\text{U}$ ,  $R(E)$  is a constant,  $Q$ , and is equal to the ratio of effective numbers of atoms multiplied by  $n$ . Above the threshold,  $R(E)$  is equal to  $(Q/n \times \sigma_{238}/\sigma_{235}) + Q$ . Once  $Q$  is subtracted from  $R(E)$  and these results are multiplied by  $n/Q$ , we obtain the ratio of the  $^{238}\text{U}/^{235}\text{U}$  fission cross sections, (Figure 1b). In

the interval from 1.75 to 4.00 MeV an average cross-section ratio of  $0.4422 \pm 0.0039$  was found.

The relative counting uncertainties become large when the fission cross-section ratio becomes small compared to the mixed chamber atom ratio,  $\eta$ . Therefore, the  $^{233}\text{U}/^{235}\text{U}$  ratio was also determined in the same experiment by including separate fission chambers containing high-purity  $^{238}\text{U}$  and high-purity  $^{235}\text{U}$ . These results were normalized to the average value of the threshold method data,  $0.4422 \pm 0.0039$  in the interval of 1.75 to 4.00 MeV (see Figures 1b and 1c). Two separate  $^{233}\text{U}$  fission chambers were used to avoid correlated errors between the two sets of measurements and to provide an experimental determination of the magnitude of the neutron flux change across the four back-to-back fission chambers. Figure 1d shows our ratio over the 0.1 to 1.5 MeV energy range.

It is possible to use the threshold method to determine normalization values for ratios involving two nonthreshold isotopes as illustrated by our  $^{233}\text{U}/^{235}\text{U}$  and  $^{239}\text{Pu}/^{233}\text{U}$  cross-section ratio measurements. For the  $^{233}\text{U}/^{235}\text{U}$  cross-section ratio measurement, we first obtained the  $^{238}\text{U}/^{235}\text{U}$  ratio (Figure 2a). The average of this ratio was  $0.3007 \pm 0.0026$  in the interval from 1.75 to 4.00 MeV. This value, together with our value for  $^{238}\text{U}/^{235}\text{U}$  cross-section ratio gave a normalization for the  $^{233}\text{U}/^{235}\text{U}$  ratio (Figure 2b). For the  $^{239}\text{Pu}/^{235}\text{U}$  cross-section ratio measurement, an auxiliary measurement of the ratio  $^{232}\text{U}/^{239}\text{Pu}$  was made using the threshold method. This data, shown in Figure 3a, yielded an average value of  $0.2895 \pm 0.0042$  in the normalization interval and was used with the  $^{236}\text{U}/^{235}\text{U}$  cross-section ratio to normalize our  $^{239}\text{Pu}/^{235}\text{U}$  ratio (Figure 3b).

Fission cross-section ratio measurements involving  $^{234}\text{U}$ ,  $^{236}\text{U}$ ,  $^{240}\text{Pu}$ ,  $^{241}\text{Pu}$ ,  $^{242}\text{Pu}$ , and  $^{244}\text{Pu}$  were also conducted at the linac. All of our normalization values were determined from the threshold-method cross-section ratios and are given in Table II, along with the values of  $\eta$  as determined by groups at LLL and the Los Alamos Scientific Laboratory. Figures 4 through 6 show our fission cross-section ratios for  $^{234}\text{U}$ ,  $^{236}\text{U}$ ,  $^{240}\text{Pu}$ ,  $^{241}\text{Pu}$ ,  $^{242}\text{Pu}$ , and  $^{244}\text{Pu}$  relative to  $^{235}\text{U}$ .

#### UNCERTAINTIES ASSOCIATED WITH THE THRESHOLD METHOD

The average cross-section ratio,  $A$ , in an energy interval is related to measured quantities by  $A = (\bar{R}/Q - 1)$ , where  $\bar{R}$  is the average of  $R(E)$  in the interval (refer to equation 1). The uncertainty in  $A$  can be conveniently written in terms of fractional errors:

$$\frac{\delta A}{A} = \left[ \left( \frac{\delta \eta}{\eta} \right)^2 + \left( \frac{A + \eta}{A} \right)^2 \left( \left( \frac{\delta R}{R} \right)^2 + \left( \frac{\delta Q}{Q} \right)^2 \right) \right]^{1/2}.$$

This error formula shows how the errors from the three measured quantities,  $\eta$ ,  $R$ , and  $Q$ , combine to give the total error in the average normalized ratio,  $A$ . The fractional errors from  $\bar{R}$  and  $Q$  are each multiplied by the term  $(A + \eta)/A$  and this factor may be considerably larger than 1 if  $\eta$  is greater than  $A$ .

For our measurements, the energy interval from 1.75 to 4.00 MeV was chosen to compute average threshold method cross-section ratios because, in this energy range, the fission ratios were generally smooth and flat. For each ratio, the energy range chosen for  $Q$  varied because the high-energy end of the interval was limited by the onset of a significant fission cross section from the threshold isotope in the mixed chamber. The low-energy end of the  $Q$  interval was generally limited by the presence of significant no-beam backgrounds.

Application of the threshold method to our data required that certain corrections be made. In the  $Q$  interval, we accounted for the subthreshold fission cross sections of the threshold isotopes. This was accomplished within the measurements by using those ratios involving the high purity fission chambers. For these measurements, the uncertainty in  $Q$  from corrections resulting from alpha-particle pileup and spontaneous fission backgrounds was negligible for all the threshold ratios, except for the  $^{244}\text{Pu}/^{239}\text{Pu}$  ratio where the error is estimated to be 0.5%. In all our ratios, the backgrounds were small fractions of the neutron-induced counts in the 1.75 to 4.00 MeV interval where  $R$  was computed and the background uncertainty in  $R$  was negligible. Out-of-time neutron backgrounds were measured using the black-resonance absorber technique and were found to contribute negligible error within the  $Q$  intervals. No correction was made for these backgrounds and it was assumed that these errors were also negligible at higher neutron energies. The neutron beam from the linac was collimated to avoid all but the thin parts of the fission chamber. We corrected the relative count rates of the mixed and pure fission chambers for neutron scattering in the aluminum foils and other chamber parts. The scattering correction was less than 0.5% in magnitude, except at the large aluminum resonances, and the uncertainty from scattering in the corrected ratio  $R(E)/Q$  was negligible.

Our measurements contain the assumption that the efficiencies for detecting fission fragments in the fission chambers are independent of neutron energy. The degree to which this assumption is realized is an especially important question in the mixed chambers. In our mixed chambers, the fissions determining  $Q$  were from the nonthreshold isotope, while the majority of the fissions determining  $R(E)$  came from the threshold isotope. We measured the energy dependence of all of our fission chamber efficiencies and our results for the uranium isotopes are available [3]. Fission-chamber pulse-height distributions were obtained simultaneously for a number of wide neutron energy bands by processing both time-of-flight and pulse-height information for each event. Comparison of these distributions at different neutron energies showed that there were energy-dependent effects that increase as the efficiency for detecting fission fragments decreases. Since our fission chambers were designed to permit good separation of fission and alpha-pileup pulses, we were able to choose the bias levels for our data so that the energy variations of the efficiencies were acceptably small (<0.5%).

An accurate determination of  $\eta$ , the atom ratio of the nonthreshold to threshold nuclide in the mixed chamber, was essential for the successful application of the threshold cross-section method. For mixtures involving two isotopes of the same element, mass spectrometry was used to determine the atom ratio. Determining the ratios involving two isotopes of different elements was more difficult, and therefore we used isotope-dilution mass spectrometry

and controlled-potential coulometry. Measurements of  $\eta$ , as determined by groups at LLL and the Los Alamos Scientific Laboratory are reported in Table II, along with their total uncertainties, expressed as standard deviations.

When preparing mixtures of different elements for the foils for the mixed chambers, special care must be taken to ensure that the mixture remains homogeneous. In some instances, the chemistry of plutonium is quite different from that of uranium, e.g., polymerization. Steps should also be taken to insure an accurate determination of  $\eta$ . In our experiment, samples were sent to various laboratories and only two of these labs were able to give atom-ratio determinations that were consistent with the quoted errors.

#### COMPARISON WITH FISSION RATIOS AT THERMAL NEUTRON ENERGY

We made a comparison for the ratios of the fissile isotopes  $^{233}\text{U}$ ,  $^{239}\text{Pu}$ , and  $^{241}\text{Pu}$  to  $^{235}\text{U}$  between our threshold method results and evaluations of thermal energy fission cross-section ratios. This was accomplished by conducting additional fission-ratios measurements at the LLL linac in the energy range from 0.01 eV to 30 keV. The low-energy results were tied to our high-energy ratios in the energy range 0.65 to 30 keV. These thermal measurements provide a cross-check on our high-energy normalization and are not an attempt to improve the thermal values. In Table III, we compare our preliminary results for fission cross-section ratios at thermal neutron energy to recent evaluations of these ratios [17,18] and our uncertainties include estimates of all identified experimental errors. The  $^{233}\text{U}/^{235}\text{U}$  ratio has a discrepancy with the evaluations which we are unable to explain at this time.

#### FURTHER COMPARISONS

Several of our fission cross-section ratios are compared over the neutron energy range including the 1.75 to 4.00 MeV normalization interval in Figure 7. The  $^{238}\text{U}/^{235}\text{U}$ ,  $^{233}\text{U}/^{235}\text{U}$ , and  $^{239}\text{Pu}/^{235}\text{U}$  ratios are discussed below.

##### The $^{238}\text{U}/^{235}\text{U}$ Fission Cross-Section Ratio

In Figure 7a, our data for the  $^{238}\text{U}/^{235}\text{U}$  fission cross-section ratio are compared to others over the neutron energy range of 1.75 to 5.5 MeV. Good agreement is found between our data and that of Jarvis [19], White and Warner [16], Meadows [11], and Poenitz [9]. The data of Stein, Smith, and Smith [15] have the same general shape as our results but their data are approximately 3.5% lower than ours.

##### The $^{233}\text{U}/^{235}\text{U}$ Fission Cross-Section Ratio

Figure 7b presents our data for the  $^{233}\text{U}/^{235}\text{U}$  fission cross-section ratio as compared to others over the energy range of 0.8 to 4.0 MeV. Our results are in good agreement with data of White and Warner [16] and of Pfeletschinger and Kaeppler [14]. The data of Meadows [8] agree in shape with our results but are about 5% higher in value.

### The $^{239}\text{Pu}/^{235}\text{U}$ Fission Cross-Section Ratio

Our  $^{239}\text{Pu}/^{235}\text{U}$  fission cross-section ratio is compared in Figure 7c with the results of White and Warner [16] and of Poenitz [12]. Good agreement is found over the energy range of 0.8 to 5.5 MeV.

Table IV contains a detailed comparison of our results with the data of White and Warner [16] at their four neutron energies: 1.0, 2.25, 5.4, and 11 MeV. Good agreement is found for the  $^{239}\text{U}/^{235}\text{U}$ ,  $^{238}\text{U}/^{235}\text{U}$ , and  $^{239}\text{Pu}/^{235}\text{U}$  ratios. Several of the remaining ratios do not agree well; however, it should be mentioned that the White and Warner results depend on alpha-decay half-lives because alpha-counting was their main assaying technique. Substituting currently accepted half-life values for those used by White and Warner brings their results into closer agreement with our data.

### CONCLUSIONS

The threshold cross-section method was successfully used to determine fission cross-section ratios of four uranium and five plutonium isotopes relative to  $^{235}\text{U}$ . We found that certain experimental errors common to past normalization methods can be eliminated or significantly reduced by use of this method. However, high-efficiency fission detectors are needed to prevent a significant energy dependence in the efficiency. This is especially true for the detector containing the isotope mixture required for the threshold method. Although the data reduction is slightly more complicated in the threshold method, one gains the advantage that the ratio of effective numbers of atoms may be determined simply and accurately.

We consider the threshold method to be a logical extension of the existing techniques and procedures, and advances in the design of neutron-producing facilities permit these methods to be more fully utilized. The threshold method is not limited to facilities producing white-neutron spectra but the simultaneous sampling of all neutron energies eliminates the effects of any slow variation in detector efficiency over the time period of the measurement.

Work on measuring fission cross-section ratios continues at LLL. Measurements of  $^{237}\text{Np}$  and  $^{241}\text{Am}$  relative to  $^{235}\text{U}$  are presently being made and in the near future,  $^{230}\text{Th}$ ,  $^{232}\text{Th}$ , and  $^{243}\text{Am}$  will also be studied. All ratios will be determined using the threshold method.

### ACKNOWLEDGMENTS

We thank R. W. Bauer, J. D. Anderson, R. L. Wagner, and F. S. Eby for their support and encouragement expressed throughout the course of this investigation. We express special thanks to R. J. Newbury and J. W. Magana for their invaluable contributions. We also thank our electronic and mechanical engineering groups for their efforts in the design and construction of our experimental apparatus as well as the linac operators and staff for their cooperation.

This work was performed under the auspices of the U.S. Energy Research & Development Administration, under contract No. W-7405-Eng-48.

## REFERENCES

1. J. W. Behrens, "Determination of Absolute Fission Cross Section Ratios Using the Method of Threshold Cross Sections," Rept. UCRL-51478, Lawrence Livermore Laboratory (1973).
2. J. W. Behrens and G. W. Carlson, "High-Energy Measurements of the Neutron-Induced Fission Cross Section Ratios Involving  $^{233}\text{U}$ ,  $^{235}\text{U}$ ,  $^{238}\text{U}$ , and  $^{239}\text{Pu}$  Using the Method of Threshold Cross Sections," Rept. UCID-16548, Lawrence Livermore Laboratory (1974).
3. G. W. Carlson, M. O. Larson, and J. W. Behrens, "Measurements of the Energy Dependence of the Efficiency of Fission Chambers," Rept. UCRL-51727, Lawrence Livermore Laboratory (1974).
4. J. W. Behrens and G. W. Carlson, "Measurement of the Neutron-Induced Fission Cross Section of  $^{241}\text{Pu}$  Relative to  $^{235}\text{U}$  from 0.001 to 30 MeV," Rept. UCRL-51925, Lawrence Livermore Laboratory (1975).
5. J. W. Behrens, G. W. Carlson, and R. W. Bauer, "Neutron-Induced Fission Cross Sections of  $^{233}\text{U}$ ,  $^{234}\text{U}$ ,  $^{236}\text{U}$ , and  $^{238}\text{U}$  With Respect to  $^{235}\text{U}$ ," in Proc. Conf. Nuclear Cross Sections and Technology, Washington, D.C., (1975), p. 591.
6. G. W. Carlson and J. W. Behrens, "Fission Cross Section Ratio of  $^{239}\text{Pu}$  to  $^{235}\text{U}$  from 0.1 to 30 MeV," Rept. UCID-16981, Lawrence Livermore Laboratory (1975).
7. J. W. Behrens, J. C. Browne, and G. W. Carlson, "Measurements of the Neutron-Induced Fission Cross Sections of  $^{240}\text{Pu}$  and  $^{242}\text{Pu}$  Relative to  $^{235}\text{U}$ ," Rept. UCID-17047, Lawrence Livermore Laboratory (1976).
8. J. W. Meadows, "The Ratio of the Uranium-233 to Uranium-235 Fission Cross Section," *Nucl. Sci. Eng.* 54, 317 (1974).
9. W. P. Poenitz and R. J. Armani, "Measurements of the Fission Cross Section Ratio of  $^{238}\text{U}$  to  $^{235}\text{U}$  from 2-3 MeV," *J. Nucl. Energy* 26, 483 (1972).
10. F. Kaeppler and E. Pfletschinger, "A Measurement of the Fission Cross Section of Plutonium-241 Relative to Uranium-235," *Nucl. Sci. Eng.* 51, 124 (1973).
11. J. W. Meadows, "The Ratio of the Uranium-238 to Uranium-235 Fission Cross Sections from 1 to 5 MeV," *Nucl. Sci. Eng.* 49, 310 (1972).
12. W. P. Poenitz, "Additional Measurements of the Ratio of the Fission Cross Sections of Plutonium-239 and Uranium-235," *Nucl. Sci. Eng.* 47, 228 (1972).
13. W. P. Poenitz, "Measurement of the Ratios of Capture and Fission Neutron Cross Sections of  $^{235}\text{U}$ ,  $^{238}\text{U}$ , and  $^{239}\text{Pu}$  at 130 to 1400 keV," *Nucl. Sci. Eng.* 40, 383 (1970).

14. E. Pfletschinger and F. Kueppeler, "A Measurement of the Fission Cross Sections of  $^{239}\text{Pu}$  and  $^{233}\text{U}$  Relative to  $^{235}\text{U}$ ," *J. Phys.* 40, 375 (1970).
15. W. E. Stein, R. K. Smith, and H. L. Smith, "Relative Fission Cross Sections of  $^{236}\text{U}$ ,  $^{238}\text{U}$ ,  $^{237}\text{Np}$ , and  $^{235}\text{U}$ ," in *Proc. Conf. Neutron Cross Sections and Technology*, Rept. CONF-680307, Washington, D.C., (1968), p. 627.
16. P. H. White and G. P. Warner, "The Fission Cross Sections of  $^{233}\text{U}$ ,  $^{234}\text{U}$ ,  $^{236}\text{U}$ ,  $^{238}\text{U}$ ,  $^{237}\text{Np}$ ,  $^{239}\text{Pu}$ ,  $^{240}\text{Pu}$ , and  $^{241}\text{Pu}$  Relative to that of  $^{235}\text{U}$  for Neutrons in the Energy Range 1-14 MeV," *J. Nucl. Energy* 21, 671 (1967).
17. H. D. Lemmel, "The Third IAEA Evaluation of the 2200 m/s and 19°C Maxwellian Neutron Data for U-233, U-235, Pu-239, and Pu-241," *Proc. Conf. Nuclear Cross Sections and Technology*, Washington, D.C., (1975), p. 286.
18. J. R. Stehn, "Thermal Data for Fissile Nuclei in ENDF/B-IV," *Trans. Amer. Nucl. Soc.*, 18, 351 (1974).
19. G. A. Jarvis, "Fission Comparison of  $^{238}\text{U}$  and  $^{235}\text{U}$  for 2.5 MeV Neutrons," Rept. LA-1571, Los Alamos Scientific Laboratory (1953).

TABLE 1  
Isotopic Analyses of High-Purity Isotopes Using Mass Spectrometry.

| Isotope           | Isotopic Composition (Mass Number)<br>(at. %) |        |        |        |        |        |       |        |        | Areal<br>Density<br>(g/m <sup>2</sup> ) |
|-------------------|---|--------|--------|--------|--------|--------|-------|--------|--------|---|
|                   | 233   | 234    | 235    | 236    | 238    | 239    | 240   | 241    | 242    |   |
| <sup>233</sup> U  | 99.99+  |        |        |        | 0.001  |        |       |        |        | 2.7                                     |
| <sup>234</sup> U  | 0.005   | 99.84  | 0.10   | 0.05   | 0.01   |        |       |        |        | 3.0                                     |
| <sup>235</sup> U  | 0.03  | 99.91  | 0.02   | 0.04   |        |        |       |        |        | 3.0                                     |
| <sup>236</sup> U  |   | 0.0025 | 99.99+ |        |        |        |       |        |        | 1.9                                     |
| <sup>238</sup> U  |   | 0.0006 |        | 99.99+ |        |        |       |        |        | 1.1                                     |
| <sup>239</sup> Pu |   |        |        |        | 99.978 | 0.020  |       |        |        | 2.0                                     |
| <sup>240</sup> Pu |   |        |        |        | 0.800  | 38.482 | 0.545 | 0.173  |        | 0.6                                     |
| <sup>241</sup> Pu |   |        |        | 0.0004 | 1.372  | 0.234  | 98.30 | 0.088  | 0.0004 | 1.9                                     |
| <sup>242</sup> Pu |   |        |        | 0.011  | 0.092  | 0.013  | 0.011 | 99.872 |        | 1.1                                     |
| <sup>244</sup> Pu |   |        |        |        | 0.004  | 0.106  | 0.074 | 1.038  | 98.578 | 1.1                                     |

TABLE II

Threshold Method Normalization Values and Measurements of  $\eta$  for Various Fission Cross-Section Ratios.

| Fission Cross-Section Ratio       | Threshold Method Normalization Value <sup>2</sup> | Determination of $\eta \pm \delta\eta$ |                        |                                    |                                 |
|-----------------------------------|---|--|------------------------|------------------------------------|---------------------------------|
|                                   |   | Mass Spectrometry                      |                        | Isotope-Dilution Mass Spectrometry | Controlled-Potential Coulometry |
|                                   |   | LLL <sup>b</sup>                       | LASL <sup>b</sup>      | LLL <sup>c,f</sup>                 | LASL <sup>c,f</sup>             |
| $^{234}\text{U}/^{235}\text{U}$   | $1.220 \pm 0.012$                                 | 0.6602<br>$\pm 0.0016$                 | 0.6621<br>$\pm 0.0016$ |                                    |                                 |
| $^{236}\text{U}/^{235}\text{U}$   | $0.7216 \pm 0.0099$                               |  | 0.4378<br>$\pm 0.0011$ | 0.4384<br>$\pm 0.0011$             |                                 |
| $^{238}\text{U}/^{235}\text{U}$   | $0.4422 \pm 0.0039$                               |  | 0.3397<br>$\pm 0.0008$ | 0.3391<br>$\pm 0.0008$             |                                 |
| $^{238}\text{U}/^{233}\text{U}$   | $0.3007 \pm 0.0026$                               |  | 0.1456<br>$\pm 0.0004$ | 0.1451<br>$\pm 0.0004$             |                                 |
| $^{238}\text{U}/^{239}\text{Pu}$  | $0.2895 \pm 0.0042$                               |  |                        | 0.1696<br>$\pm 0.0008$             | 0.1686<br>$\pm 0.0004$          |
| $^{238}\text{U}/^{240}\text{Pu}$  | $0.3233 \pm 0.0065$                               |  |                        | 0.1743<br>$\pm 0.0008$             | 0.1716<br>$\pm 0.0004$          |
| $^{238}\text{U}/^{241}\text{Pu}$  | $0.3484 \pm 0.0055$                               |  |                        | 0.2892<br>$\pm 0.0013$             | 0.2904<br>$\pm 0.0006$          |
| $^{242}\text{Pu}/^{239}\text{Pu}$ | $0.7342 \pm 0.0095$                               | 0.3361<br>$\pm 0.0008$                 |                        |                                    | 0.3353<br>$\pm 0.0034$          |
| $^{244}\text{Pu}/^{239}\text{Pu}$ | $0.6406 \pm 0.0101$                               | 0.4293<br>$\pm 0.0011$                 |                        |                                    | 0.4270<br>$\pm 0.0043$          |

<sup>2</sup>Over the normalization energy interval 1.75-4.00 MeV. Errors indicate total uncertainties expressed as standard deviations.

<sup>b</sup>Analyzed by R. S. Newbury, Lawrence Livermore Laboratory.

<sup>c</sup>As determined by J. H. Cappis, Los Alamos Scientific Laboratory.

<sup>d</sup>Determined by J. E. Rein and G. R. Waterbury, Los Alamos Scientific Laboratory.

<sup>e</sup>Determined by J. W. Nagana and J. E. Harrar, Lawrence Livermore Laboratory. Direct weighing was used on the  $^{242}\text{Pu}$  and  $^{244}\text{Pu}$  samples.

<sup>f</sup>Assays performed at intermediate steps in the fission foil preparation. These assays indicate that gross errors were not present in the preparation technique.

TABLE III

Comparison to Thermal Fission Cross-Section Ratios Relative to  $^{235}\text{U}$ .

| Fission Cross-Section Ratio      | Present Work  |                   | Lemmel <sup>a</sup> |                   | Difference         |               | Stehn <sup>b</sup> |                    | Difference    |                   |
|----------------------------------|---------------|-------------------|---------------------|-------------------|--------------------|---------------|--------------------|--------------------|---------------|-------------------|
|                                  | Thermal Ratio | Percent Error (%) | Thermal Ratio       | Percent Error (%) | $\Delta_{a,c}$ (%) | Thermal Ratio | Percent Error (%)  | $\Delta_{b,c}$ (%) | Thermal Ratio | Percent Error (%) |
| $^{233}\text{U}/^{235}\text{U}$  | 0.879         | $\pm 1.6$         | 0.908               | $\pm 0.3$         | +3.2               |               | 0.911              |                    | +3.5          |                   |
| $^{239}\text{Pu}/^{235}\text{U}$ | 1.279         | $\pm 2.4$         | 1.275               | $\pm 0.3$         | -0.3               |               | 1.267              |                    | -0.9          |                   |
| $^{241}\text{Pu}/^{235}\text{U}$ | 1.772         | $\pm 2.5$         | 1.740               | $\pm 0.7$         | -1.8               |               | 1.722              |                    | -2.9          |                   |

<sup>a</sup>H. D. Lemmel (1975). See Reference 17.<sup>b</sup>J. R. Stehn (1974). See Reference 18.<sup>c</sup> $\Delta \equiv \frac{\text{Evaluated Value} - \text{Present Work}}{\text{Evaluated Value}} \times 100\%$ .

TABLE IV

Comparison of Present Work With White and Warner.<sup>a</sup>

| Fission Cross-Section Ratio      | Neutron Energy (MeV)      |                                  |                   |                           |                      |                   |                           |                      |                   |                           |                      |                   |
|----------------------------------|---------------------------|----------------------------------|-------------------|---------------------------|----------------------|-------------------|---------------------------|----------------------|-------------------|---------------------------|----------------------|-------------------|
|                                  | 1.0                       |                                  |                   | 2.25                      |                      |                   | 5.4                       |                      |                   | 14.1                      |                      |                   |
|                                  | Present Work <sup>b</sup> | $W/W^2, c$                       | $\Delta^b$ (%)    | Present Work <sup>b</sup> | $W/W^2, c$           | $\Delta^b$ (%)    | Present Work <sup>b</sup> | $W/W^2, c$           | $\Delta^b$ (%)    | Present Work <sup>b</sup> | $W/W^2, c$           | $\Delta^b$ (%)    |
| $^{233}\text{U}/^{235}\text{U}$  | 1.514<br>$\pm 0.022$      | 1.504<br>$\pm 0.030$             | +0.7<br>$\pm 0.7$ | 1.483<br>$\pm 0.021$      | 1.454<br>$\pm 0.029$ | +2.0<br>$\pm 2.0$ | 1.410<br>$\pm 0.026$      | 1.362<br>$\pm 0.027$ | +3.4<br>$\pm 3.4$ | 1.076<br>$\pm 0.025$      | 1.079<br>$\pm 0.022$ | -0.3<br>$\pm 0.3$ |
| $^{234}\text{U}/^{235}\text{U}$  | 0.910<br>$\pm 0.018$      | 0.953<br>$\pm 0.019$             | -4.7<br>$\pm 4.7$ | 1.181<br>$\pm 0.021$      | 1.127<br>$\pm 0.023$ | +4.6<br>$\pm 4.6$ | 1.213<br>$\pm 0.025$      | 1.206<br>$\pm 0.024$ | +0.6<br>$\pm 0.6$ | 0.972<br>$\pm 0.034$      | 0.956<br>$\pm 0.019$ | +1.6<br>$\pm 1.6$ |
| $^{236}\text{U}/^{235}\text{U}$  | 0.306<br>$\pm 0.008$      | 0.278<br>$\pm 0.006$             | +9.2<br>$\pm 9.2$ | 0.706<br>$\pm 0.015$      | 0.655<br>$\pm 0.015$ | +7.2<br>$\pm 7.2$ | 0.800<br>$\pm 0.013$      | 0.765<br>$\pm 0.018$ | +4.4<br>$\pm 4.4$ | 0.775<br>$\pm 0.015$      | 0.738<br>$\pm 0.015$ | +4.8<br>$\pm 4.8$ |
| $^{238}\text{U}/^{235}\text{U}$  | 0.0141<br>$\pm 0.0005$    | N.M. <sup>d</sup><br>$\pm 0.006$ |                   | 0.426<br>$\pm 0.006$      | 0.427<br>$\pm 0.009$ | -0.2<br>$\pm 0.2$ | 0.535<br>$\pm 0.008$      | 0.528<br>$\pm 0.011$ | +1.3<br>$\pm 1.3$ | 0.557<br>$\pm 0.010$      | 0.549<br>$\pm 0.011$ | +1.4<br>$\pm 1.4$ |
| $^{239}\text{Pu}/^{235}\text{U}$ | 1.438<br>$\pm 0.026$      | 1.435<br>$\pm 0.029$             | +0.2<br>$\pm 0.2$ | 1.525<br>$\pm 0.028$      | 1.520<br>$\pm 0.030$ | +0.3<br>$\pm 0.3$ | 1.592<br>$\pm 0.033$      | 1.575<br>$\pm 0.032$ | +1.1<br>$\pm 1.1$ | 1.149<br>$\pm 0.029$      | 1.163<br>$\pm 0.023$ | -1.2<br>$\pm 1.2$ |
| $^{240}\text{Pu}/^{235}\text{U}$ | 1.245<br>$\pm 0.028$      | 1.154<br>$\pm 0.023$             | +7.3<br>$\pm 7.3$ | 1.340<br>$\pm 0.032$      | 1.261<br>$\pm 0.025$ | +5.9<br>$\pm 5.9$ | 1.409<br>$\pm 0.035$      | 1.409<br>$\pm 0.028$ | 0.0<br>$\pm 0.0$  | 1.093<br>$\pm 0.033$      | 1.047<br>$\pm 0.021$ | +4.2<br>$\pm 4.2$ |
| $^{241}\text{Pu}/^{235}\text{U}$ | 1.291<br>$\pm 0.027$      | 1.356<br>$\pm 0.027$             | -5.0<br>$\pm 5.0$ | 1.262<br>$\pm 0.027$      | 1.325<br>$\pm 0.026$ | -5.0<br>$\pm 5.0$ | 1.273<br>$\pm 0.035$      | 1.290<br>$\pm 0.026$ | -1.3<br>$\pm 1.3$ | 1.070<br>$\pm 0.038$      | 1.119<br>$\pm 0.022$ | -4.6<br>$\pm 4.6$ |

<sup>a</sup>P. H. White and G. P. Warner (1967). See Reference 16.<sup>b</sup> $\Delta \equiv \frac{(\text{Present Work}) - (\text{Ref. 16})}{(\text{Present Work})} \times 100\%$ .<sup>c</sup>Errors are one standard deviation of total uncertainties.<sup>d</sup>Not Measured.

#### FIGURE CAPTIONS

Figure 1. Fission cross-section ratio of  $^{238}\text{U}$  to  $^{235}\text{U}$ : statistical error bars are shown. (a) Threshold method ratio of the mixed chamber to the pure chamber rate file. (b) Threshold method ratio (+) compared to the ratio obtained from the high-purity isotope chambers (continuous line). (c) Ratio obtained from the high-purity chambers, normalized to  $0.4422 \pm 0.0039$  from 1.75 to 4.00 MeV. (d) Ratio from the high-purity chambers from 0.1 to 1.5 MeV.

Figure 2. Fission cross-section ratios: statistical error bars are shown for each point. (a) Threshold method ratio of  $^{238}\text{U}$  to  $^{233}\text{U}$ . (b) Ratio of  $^{233}\text{U}$  to  $^{235}\text{U}$ , normalized to  $1.471 \pm 0.018$  from 1.75 to 4.00 MeV.

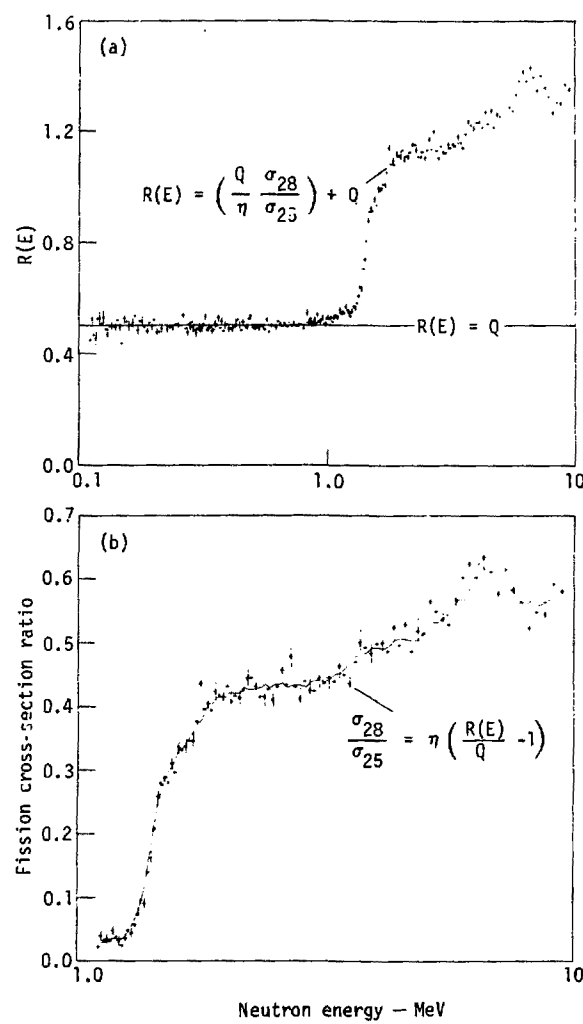
Figure 3. Fission cross-section ratios: statistical error bars are shown for each point. (a) Threshold method ratio of  $^{238}\text{U}$  to  $^{239}\text{Pu}$ . (b) Ratio of  $^{239}\text{Pu}$  to  $^{235}\text{U}$ , normalized to  $1.527 \pm 0.026$  from 1.75 to 4.00 MeV.

Figure 4. Fission cross-section ratios: statistical error bars are shown for each point. (a) Ratio of  $^{234}\text{U}$  to  $^{235}\text{U}$ , normalized to  $1.220 \pm 0.012$ . (b) Ratio of  $^{236}\text{U}$  to  $^{235}\text{U}$ , normalized to  $0.7216 \pm 0.0099$ .

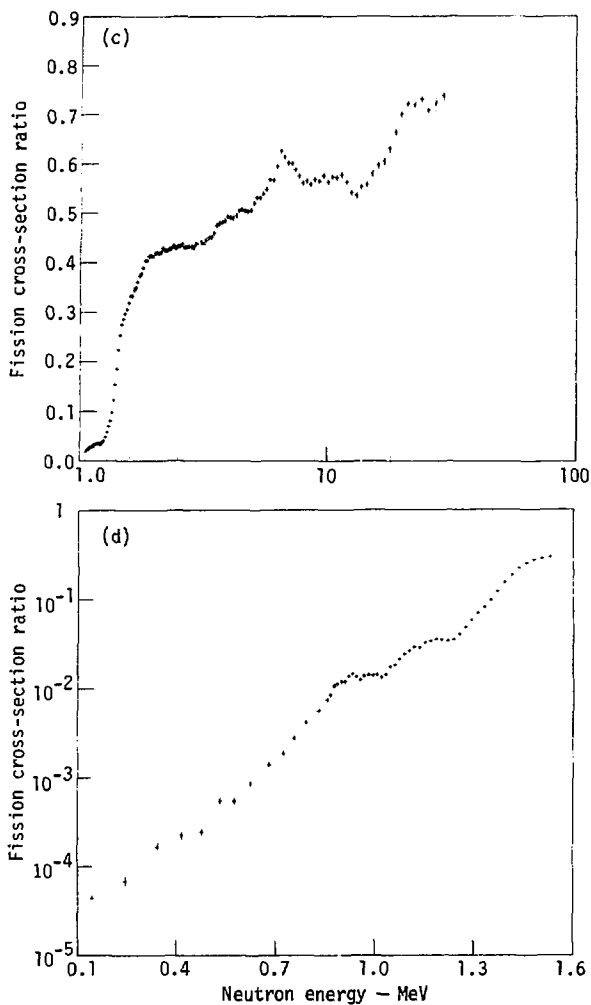
Figure 5. Fission cross-section ratio of  $^{241}\text{Pu}$  to  $^{235}\text{U}$ , normalized to  $1.269 \pm 0.023$  from 1.75 to 4.00 MeV. Statistical error bars are shown for each point.

Figure 6. Fission cross-section ratios: statistical error bars are shown for each point. (a) Ratio of  $^{240}\text{Pu}$  to  $^{235}\text{U}$ , normalized to  $1.367 \pm 0.030$ . (b) Ratio of  $^{242}\text{Pu}$  to  $^{235}\text{U}$ , normalized to  $1.121 \pm 0.024$ . (c) Ratio of  $^{244}\text{Pu}$  to  $^{235}\text{U}$ , normalized to  $0.9782 \pm 0.023$ .

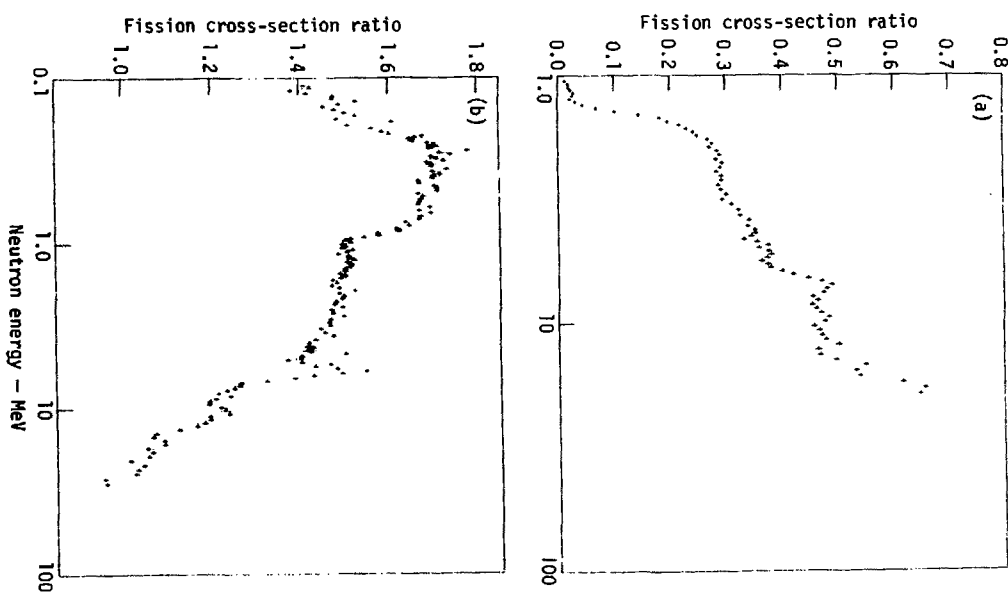
Figure 7. Fission cross-section ratios. Present work is represented by (+) and letter codes indicate the work of other investigators. Error bars represent the total uncertainties, expressed as standard deviations. (a) Ratio of  $^{238}\text{U}$  to  $^{235}\text{U}$  from 1.8 to 4.0 MeV. (b) Ratio of  $^{233}\text{U}$  to  $^{235}\text{U}$  from 0.8 to 4.0 MeV. (c) Ratio of  $^{239}\text{Pu}$  to  $^{235}\text{U}$  from 0.8 to 5.5 MeV.



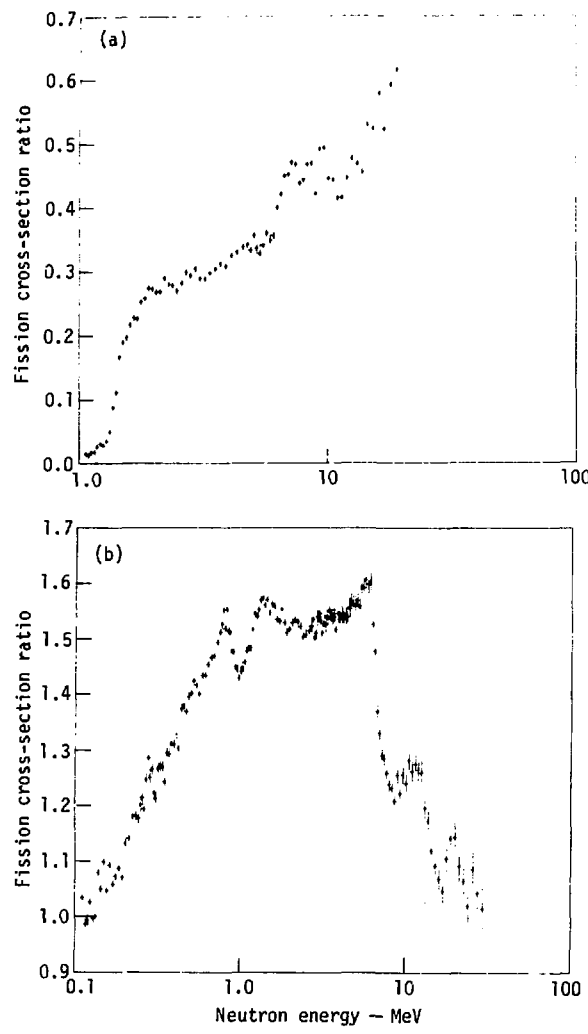
Behrens - Fig. 1



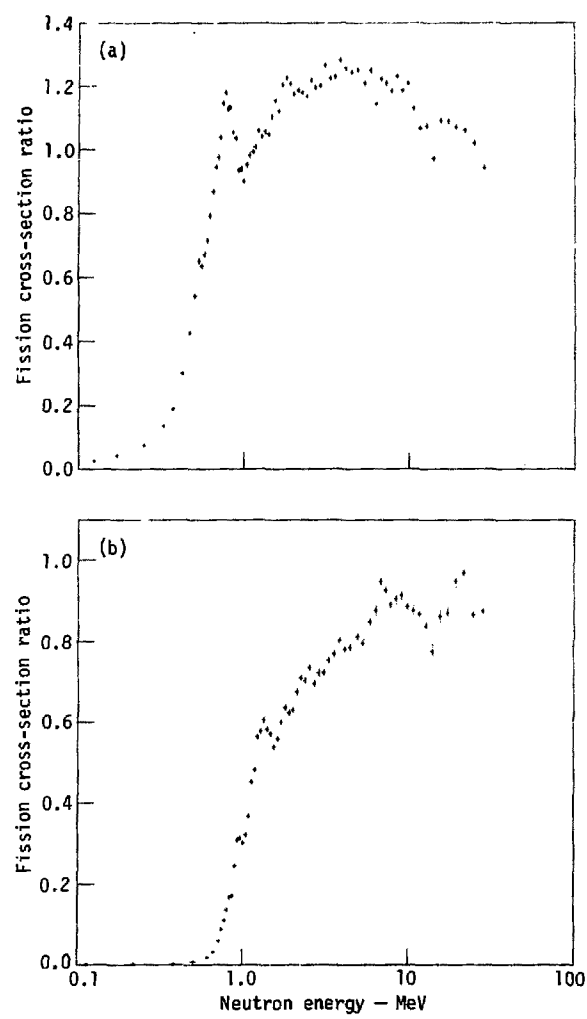
Behrens - Fig. 1  
Continued



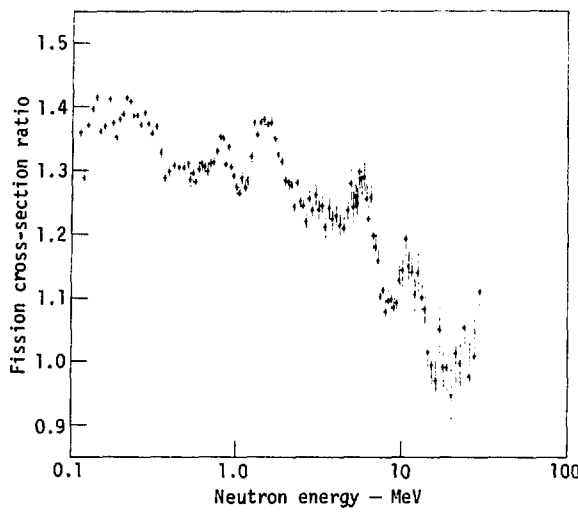
Behrens - Fig. 2



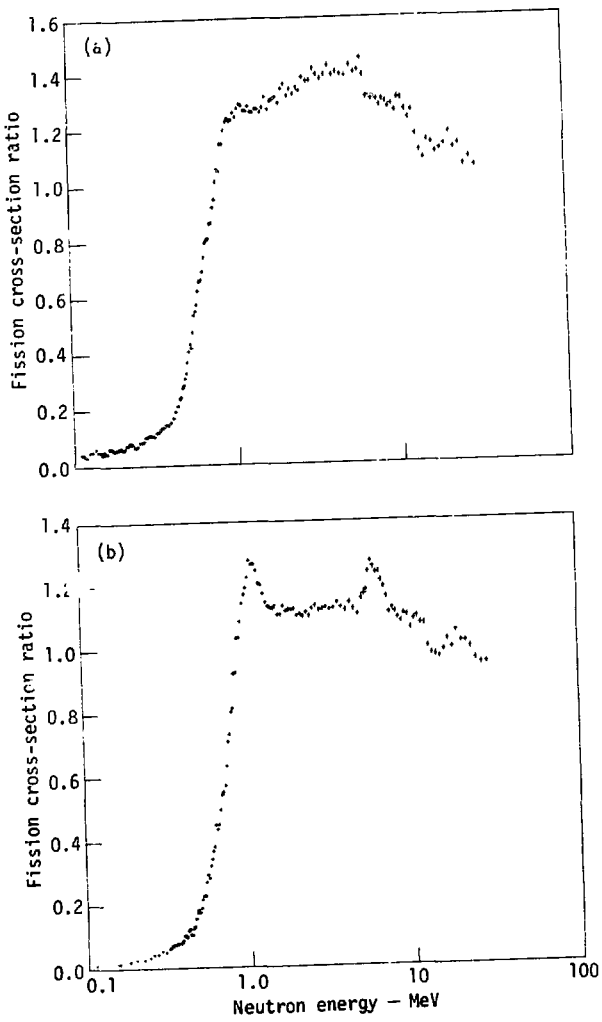
Behrens - Fig. 3



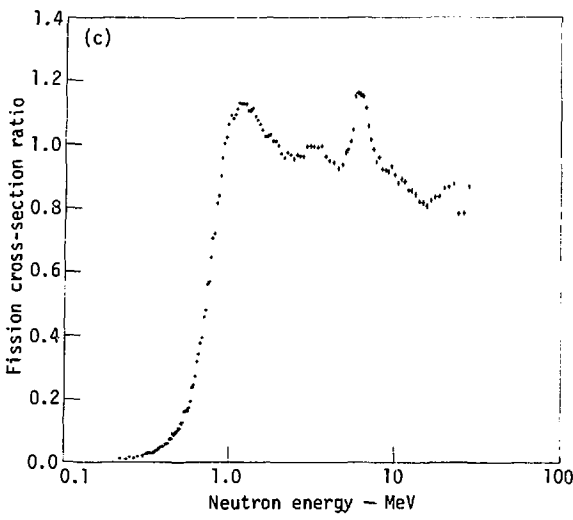
Behrens - Fig. 4



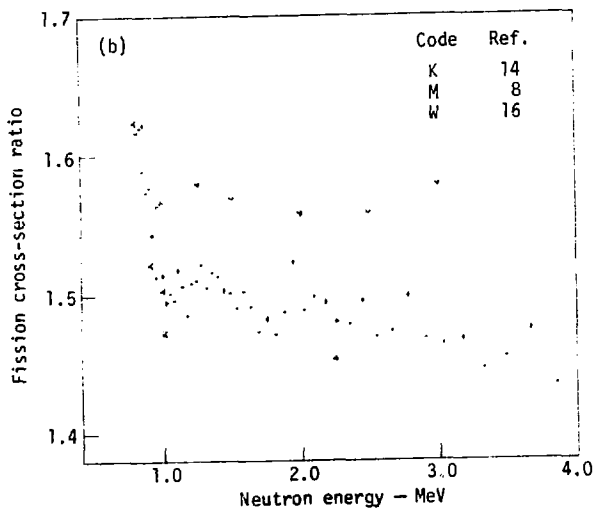
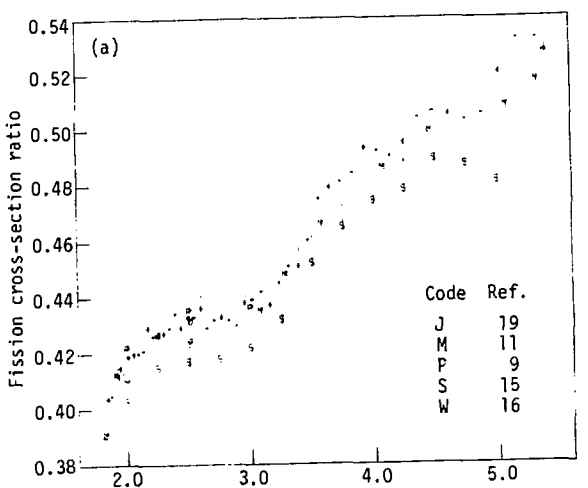
Behrens - Fig. 5



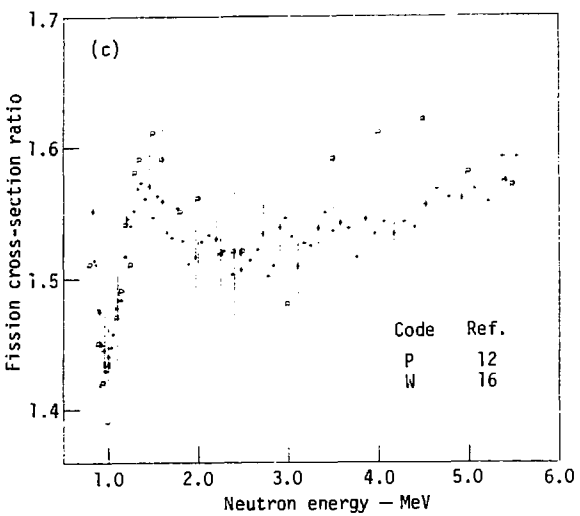
Behrens - Fig. 6



Behrens - Fig. 6  
Continued



Behrens - Fig. 7



Behrens - Fig. 7  
Continued